Tunneling through Weak Interactions: Comparison of Through-Space-, H-Bond-, and Through-Bond-Mediated Tunneling

Westin Kurlancheek[†] and Robert J. Cave*

Department of Chemistry, Harvey Mudd College, 301 Platt Boulevard, Claremont, California 91711

Received: July 20, 2006; In Final Form: October 18, 2006

Results from ab initio electronic structure theory calculations on model systems allow for the detailed comparison of tunneling through covalently bonded contacts, hydrogen bonds, and van der Waals contacts. Considerable geometrical sensitivity as well as an exponential distance dependence of the tunneling is observed for tunneling through various nonbonded contacts. However, the fundamental result from the present study is that at most a modest difference is observed between tunneling mediated by H-bonds and tunneling mediated by van der Waals contacts at typical distances for each type of interaction. These results are considered in relation to the pathways model of Beratan and Onuchic, and implications for understanding long-range tunneling in biological systems are discussed.

1. Introduction

Electron-transfer reactions play an important role in a variety of biological processes.[1–10] Understanding at a fundamental level of several features of biological electron transfers would be desirable in the design of synthetic systems that mimic their efficiencies and directionality. For example, the initial charge-transfer steps in photosynthetic electron transfer are quite rapid but lose little of the initiating photon's energy.[10] In the mitochondrial electron transport chain there are several steps that expend little energy shuttling the electron between sites, whereas others are designed to expend energy in the service of pumping protons.[1] In each of these cases the electron transfers are quite specific and occur over considerable distances.

The works of Marcus,[11] Hush,[12] Levich,[13] Dogonadze,[14] and Jortner[15,16] have provided a theoretical framework for understanding many of the features of these and other electron-transfer processes. In the limit of high temperature and weakly interacting donor and acceptor, the rate of electron transfer can be written as[17]

$$k_{et}(R) = \frac{2\pi}{\hbar} |H_{DA}|^2 \left(\frac{1}{4\pi\lambda k_B T}\right)^{1/2} \exp(-\Delta G^{\ddagger}/k_B T) \quad (1)$$

The principal distance- and orientation-dependent portion of the rate expression (eq 1) is the electronic coupling element, H_{DA}. As a result, considerable effort has been expended to understand the dependence of the coupling element on the nature of the donor, acceptor, bridging medium, and relative energetics of the electron transfer.

The pathways model of Beratan and Onuchic[18–22] provided an overarching construct in which to consider how the medium between the donor and acceptor might affect the electronic coupling element. The model's importance to the discipline of biological electron transfer is difficult to overestimate. The pathways model has provided a coarse-grained distinction between various bridging "contacts" (through-bond, H-bond, through-space, or van der Waals contacts and, more recently, through-water) and has helped guide and focus experimental efforts in a variety of groups.[8,23] The essence of the pathways model is that through-bond connections, being intrinsically stronger than van der Waals (through-space) contacts, should yield considerably weaker decay with distance for electron or hole tunneling.[19,24] Thus, when possible, tunneling should occur through bonded connections. However, when bonded connections represent a particularly circuitous route between the donor and acceptor, it is possible to tunnel through van der Waals contacts or, even, through interstitial waters. H-bond tunneling was parametrized as having a much weaker decay than van der Waals contacts (equivalent to two covalent bonds at a normal H-bond distance), whereas the through-space decay (i.e., van der Waals decay) was equivalent to decay through about nine covalent bonds at a normal methyl–methyl van der Waals contact distance. In part, the genius of this approach was the neglect of specific chemical details in the name of developing a general sense of distance dependence in biological electron transfers. It also had the distinct merit of allowing direct predictions for relative rates between different pathways in a protein. Beratan and Onuchic emphasized that their model is simplified—it neglects interference between pathways, treats all bonded connections as equivalent, and ignores orientation dependence except in an average sense.[24,25] Nevertheless, it has helped set the parameters of the discussion of distance dependence in biological electron transfers for the past 20 years.

More detailed treatments of tunneling in model systems as well as actual systems of biological relevance have supported many of the ideas inherent in the pathways model.[26–45] Quite detailed studies of tunneling in alkane chains have illuminated the nature of interference effects,[26–30,45] but still validate the treatment of chemical units as leading to (nearly) equivalent decays with distance as the chain between donor and acceptor becomes elongated. A number of experimental studies have also investigated the impact of nonbonded contacts on the electronic coupling element and seen significant contributions to the coupling from weak interactions. For example, early studies by Beitz and Miller[46–48] and more recent work by the Winkler and

* Author to whom correspondence should be addressed (e-mail Robert_Cave@hmc.edu).

† Present address: Department of Chemistry, Room 419, Latimer Hall, University of California, Berkeley, CA 94720.

Tunneling through Weak Interactions

J. Phys. Chem. A, Vol. 110, No. 51, 2006 **14019**

Gray group[49,50] have shown that tunneling through solvent glasses (where nonbonded contacts must play a role) decays more rapidly than through-bond tunneling, but still presents a viable route for long-range electron transfer. In addition, a number of groups have developed synthetic model systems that allow for the examination of through-space and through-solvent tunneling. Zimmt et al. have explored tunneling mediated by solvent in their C-clamp molecules, where the through-bond tunneling pathway is sufficiently long that direct through-space tunneling between donor and acceptor becomes competitive.[51−54] Paddon-Row and co-workers have synthesized analogous systems in which covalently attached pendent groups are interposed between donor and acceptor and significant effects on the coupling are observed.[55]

Therien and co-workers have studied the effects of H-bonds on the coupling between a donor and acceptor and have found that the coupling through H-bonds is comparable to that through covalent bonds in their system, which is consistent with the pathways model.[23] Winkler and Gray have also suggested that the H-bond network in aqueous sulfuric acid glasses may contribute to the higher-than-expected tunneling rates they observed in these systems.[8]

A number of theoretical studies have also addressed how nonbonded contacts affect the electronic coupling between a donor and an acceptor. Newton studied tunneling through methanes and water molecules and found decay constants similar to those observed in straight-chain alkanes.[56] His results also indicated that tunneling through H-bonds was competitive to through-bond tunneling in a set of model compounds. We have investigated tunneling through water using simple donors and acceptors and solvent configurations generated using molecular dynamics methods as well as model solvent geometries.[57,58] The overall results were consistent with experimental results for tunneling through water, but somewhat surprising results were obtained using high-level ab initio wavefunctions to treat the model water geometries. There it was found that coupling through a water dimer was largely insensitive to the relative orientation of the waters. That is, H-bonded configurations provided no larger values of the coupling than some van der Waals contacts (having no conventional H-bonds). Furthermore, in comparisons of tunneling through van der Waals contacts and through-bond tunneling for straight-chain alkanes we found that through-space tunneling, although more rapidly decaying than through-bond tunneling, was not nearly as weak as one would expect on the basis of the pathways parametrization.

There is experimental precedent for somewhat surprisingly large through-space/van der Waals coupling.[59] Tezcan et al. examined interprotein electron transfer in crystals and found robust coupling despite the fact that the faces of the proteins along the line of centers between donor and acceptor presented largely non-H-bonded contacts through which to tunnel. In addition, in the studies of their C-clamp molecules, Zimmt et al. showed that intervening solvent could have marked effects on the coupling, further demonstrating that van der Waals contacts can play an integral role in mediating the coupling.[54] To the best of our knowledge, however, no theoretical studies have made direct comparisons of through-bond, H-bond, and through-space tunneling in systems where ab initio electronic structure techniques could be used to provide accurate assessments of the relative strengths of these couplings. Our goal in the present paper is to fill this gap and provide the theoretical results necessary to make these comparisons.

The results presented in the following sections will elucidate significant orientation effects in the tunneling through weak

TABLE 1: Optimized and Idealized Bond Lengths for D−B−A Systems

atom type	optimized distance (Å)	idealized distance (Å)
R_{C-C}	1.52−3	1.54
R_{C-N}	1.48	1.47
R_{C-H}	1.09	1.07
R_{C-P}		1.87
R_{C-O}	1.42−3	1.43
R_{N-H}	1.02	1.00
R_{P-H}		1.40
R_{O-H}	0.97−8	0.96
R_{Si-H}		1.47
R_{C-Si}		1.94

interactions. They will also show that the conclusions we draw are relatively insensitive to energetic effects. However, the fundamental result will be that, at least for the model systems treated here, there is no significant difference between tunneling through H-bonded or van der Waals contacts (at the inter-heavy-atom distances appropriate to each). We will further show that the strengths of tunneling through H-bond contacts and van der Waals contacts are intermediate between the pathways estimates for each of these types of contact.

It should be emphasized what we *do not seek to accomplish* at the outset. This is not an attempt to reparametrize the pathways model in the hopes of obtaining more accurate (but still coarse-grained) coupling elements from such a model. In the end, for treatments of biological systems it is now possible to use more detailed methods to probe the coupling element. Furthermore, it is not an attempt to somehow suggest that the pathways model was misguided because it treated tunneling via averaged parameters or because interference effects are neglected. It is, however, intended as a possible *qualitative corrective*. It is possible that the many successes of the model have led to the de facto adoption of the less tested aspect of the model, namely, that H-bonds mediate tunneling significantly better than other weak interactions. Although this may be the case in some systems, our calculations strongly argue that for the present model systems there is no significant difference between these two types of weak interactions.

The remainder of the paper is organized as follows. In section 2 we discuss the theoretical methods used and the model systems we treat. In section 3 we present our results for through-bond-, through-space-, and H-bond-mediated tunneling. In section 4 we discuss our results, and we present our conclusions in section 5.

2. Theoretical Methods

The systems treated here are of the form D−B−A, where D is the electron donor, A is the electron acceptor, and B is the bridge that may contain through-bond, van der Waals, or hydrogen-bond contacts. We exclusively consider tunneling in the +1 cation state of these systems, assuming a single electron transfer from D to A. The geometry of these structures, in most cases, was an idealized, model molecular geometry created in the GaussView environment.[60] However, several systems possessing hydrogen-bond contacts were fully optimized using density functional theory[61] with the B3LYP functional[62] and the 6-31G* basis.[63−69] The idealized structures we consider are built under the assumption that all atoms follow VSEPR-like geometrical rules. The default bond lengths in the GaussView package were used for these idealized structures and are shown in Table 1 along with the values obtained in the optimizations associated with the hydrogen-bonded structures.

Four donor/acceptor groups were used with the majority of the calculations done using the −CH₂ radical for the donor/

SCHEME 1: One of the Geometry Variations Examined in This Study
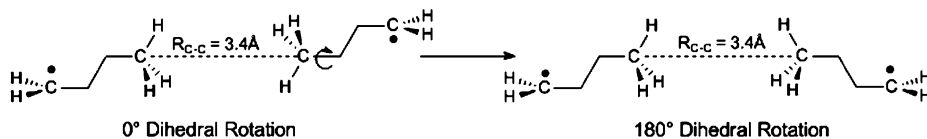
acceptor group. Other donor/acceptor groups used in this study include the $-SiH_2$ radical, $-NH_2$, and $-PH_2$. For all of the systems presented, the donor group is always identical to the acceptor group (other than having a different number of electrons). The CH_2 and SiH_2 D/A groups had planar geometries, whereas the NH_2 and PH_2 D/A groups were trigonal pyramidal.

We consider two general types of systems, so-called "connected" and "disconnected" systems. The connected systems maintain a single all-trans covalent bonding network (all CH_2 units) between the donor and acceptor. The disconnected systems in idealized geometries are formed from the connected systems by deleting two central carbons (with their associated H atoms), yielding two subsystems having a total of $n - 2$ heavy atoms. Thus, each subunit maintains an all-trans structure. For investigation of tunneling through van der Waals contacts the inner portions of the (now) two chains are terminated with H atoms at the standard C−H bond length and bond angle. The two chains are either utilized in this orientation (Tables 3 and 4) or reoriented to a head-on configuration as in Tables 5−7. For heteroatom termination (to investigate H-bond contacts or other van der Waals contacts) we substitute the group of interest (OH, NH_2, F = R in place of the central CH_3) on one or both of the disconnected chains formed for investigation of the methyl−methyl van der Waals interactions. For the optimized disconnected (nonidealized) geometries we create fragments as described above, but the molecular geometries are obtained from a geometry optimization using B3LYP and the 6-31G* basis.

In naming the fully connected systems we denote them by the number of heavy atoms in the chain, inclusive of the donor and acceptor. In denoting the disconnected systems, we name them on the basis of the *parent system* from which the central atoms were deleted. Thus, a disconnected system containing 8 heavy atoms arises from a connected system having 10 heavy atoms and is denoted as an $n = 10$ disconnected system. Except for a set of calculations referred to in section 4, *all results are based on n = 10 disconnected systems, that is, they contain 8 heavy atoms, 4 in each subunit.*

We also included examples of orientation effects by changing various angles that define the relative orientation of the two fragments in the disconnected system. For example, in Scheme 1 we illustrate one such rotation where an entire fragment is rotated with respect to the second fragment. This set of calculations starts at the 0° rotation geometry, with intervening calculations at every 30°, ending at the 180° rotation geometry. Other orientations are discussed in section 3.

For all of the systems in this study, adiabatic wavefunctions were used to calculate the electronic coupling element, H_{DA}. In some cases the systems considered had symmetry constraints relating the donor and acceptor. When symmetry was present, H_{DA} was calculated simply as half the energy difference between the initial and final states[70] (eq 2)

$$H_{DA} = \frac{\Delta E_{12}}{2} \qquad (2)$$

We used multiconfiguration self-consistent field (MCSCF)/6-31G*, unrestricted Hartree−Fock (UHF)/6-31G*, and unrestricted coupled cluster singles and doubles (UCCSD)/6-31G*

methods to calculate H_{DA} for these cases. For asymmetrical systems eq 2 does not hold, and it becomes necessary to use the generalized Mulliken−Hush method[71−74] or related approaches to calculate H_{DA}. In these cases we used MCSCF/6-31G*, CI/6-31G*, and EOM-CCSD/6-31G* wavefunctions[75,76] to calculate the necessary components (transition dipole moments, dipole moments, and energy difference between the reactant and product states) for the generalized Mulliken−Hush theory. The MCSCF wavefunction used was a two-state, state-averaged (SA) MCSCF (two-state SA-MCSCF). The two configurations correspond to the cation doublet ground state and its first excited state, where one electron from the donor has been transferred to the acceptor. Unless otherwise noted, we used a 6-31G* basis for these calculations. When the donor/acceptor is from group IV, the MCSCF is a one-electron, two-orbital two-state SA-MCSCF, whereas for donor/acceptors from group V a three-electron, two-orbital two-state SA-MCSCF calculation was performed. EOM-CCSD/6-31G* calculations were used to test the effects of including correlation on the electronic coupling element. (We used a symmetrized transition dipole moment as in previous calculations.)[58] Similar to the SA-MCSCF calculations, the EOM-CCSD calculations produced two states, which include the cation ground state and the first excited state, where one electron from the donor has been transferred to the acceptor. Correlation effects were also examined using first-order and second-order CI wavefunctions. The CI results supported those obtained using the EOM-CCSD method, and as a result we do not report them here. The calculations in this study have been performed using Gaussian 98[77] and 03[78] (UHF, UCCSD, and optimizations using B3LYP) GAMESS[79] (SA-MCSCF and CI), and ACES II[80] (EOM-CCSD) software packages.

To compare our results with the pathways model, the H_{DA} values need to be converted into decay constants for through-bond, through-space, and H-bond contacts (ϵ_C, ϵ_S, and ϵ_H, respectively.) Following our previous results, the decay constant for a through-bond contact is calculated simply using the ratio of two H_{DA} values for two fully connected systems.[70]

$$\epsilon_C^2 = \frac{H_{DA}^{n+2}}{H_{DA}^n} \qquad (3)$$

For the disconnected systems (either H-bond or van der Waals contacts) the decay constant for through-space decay (ϵ_S) or H-bond decay (ϵ_H) is related to the ratio of the disconnected and the connected chain couplings via[70]

$$\epsilon_S(R) = \frac{H_{DA,disconnected,vanderWaals}^n}{H_{DA,connected}^n} \epsilon_C^3$$

$$\epsilon_H(R) = \frac{H_{DA,disconnected,H-bonded}^n}{H_{DA,connected}^n} \epsilon_C^3 \qquad (4)$$

The above expressions can be understood on a qualitative basis in the following way. The transition from connected to discon-

Tunneling through Weak Interactions

J. Phys. Chem. A, Vol. 110, No. 51, 2006 **14021**

TABLE 2: H_{DA} (eV) Values Obtained Using Equation 1 for Connected Chain Carbon Donor/Acceptor Systems

n	SA-MCSCF/6-31G*	UHF/6-31G*	UCCSD/6-31G*
4	4.00E−01	5.11E−01	4.26E−01
6	2.19E−01	3.07E−01	2.60E−01
8	9.03E−02	1.47E−01	1.48E−01
10	3.13E−02	6.13E−02	7.44E−02
12	1.14E−02	2.66E−02	3.90E−02

TABLE 3: ϵ_C Values Calculated Using Equation 2 for Connected Carbon Donor/Acceptor Systems

$n/n+2$	SA-MCSCF/6-31G*	UHF/6-31G*	UCCSD/6-31G*
4/6	0.74	0.74	0.78
6/8	0.64	0.69	0.75
8/10	0.59	0.65	0.71
10/12	0.60	0.66	0.72
12/14	0.60	0.66	0.73
ϵ_C^{av}	0.64	0.69	0.74

nected system of a given n implies removal of two heavy atoms (i.e., three covalent bonds and therefore a factor of ϵ_C^3) and substitution of either a van der Waals (ϵ_S) or H-bond (ϵ_H) contact. Thus, multiplication of the ratio of coupling elements by ϵ_C^3 should yield the van der Waals or H-bond decay constant. However, because through-space and hydrogen-bond contacts can occur over a variety of distances, we explicitly note their distance dependence in the above expressions (implying that $H_{DA,disconnected}$ is also dependent on the distance between the two central groups of the disconnected chains). This distance dependence is expected to be approximately exponential. We calculated the distance dependence by varying the distance between the two central heavy atoms from 2.875 to 4.875 Å and at each distance calculated H_{DA}. From these calculations, the exponential dependence as a function of distance between the two contacts was derived via a least-squares fit to the data.

A variety of basis sets were used on a representative number of systems to test the dependence of H_{DA} on basis set. These include the 6-31++G*, 6-311G(d,p), and 6-311++G(d,p) sets.[81−84]

3. Results

Table 2 contains values of the electronic coupling element, H_{DA}, for the connected chain systems with CH_2 donor/acceptor pairs using SA-MCSCF, UHF, and UCCSD wavefunctions. The geometries used were symmetrical all-trans arrangements with idealized bond distances (see Table 1). Because the connected chains were symmetrical, eq 2 was used to calculate H_{DA}. Table 2 provides a direct comparison of coupling between methods that neglect correlation (SA-MCSCF and UHF) and include it (UCCSD). From these results, one can conclude that all of the H_{DA} values are of comparable size, that the MCSCF results decay somewhat more rapidly than the UHF or UCCSD values, and that correlation has little impact on the size of the electronic coupling element.

To compare our results to the pathways model results, the magnitudes of H_{DA} seen in Table 2 are used to calculate to ϵ_C values via eq 3. Table 3 presents these results and also includes the arithmetic mean of the ϵ_C values for each method (geometric mean is quite similar). This ϵ_C^{av} will be used to compare to the pathways model result and will also be used for the calculation of ϵ_S and ϵ_H via eq 4. Beyond the $n = 6$ chain, the ϵ_C values stabilize and the magnitudes appear in the order MCSCF < UHF < UCCSD. Despite these minor differences, all three methods produce very similar ϵ_C values. Given this similarity, we focus on SA-MCSCF results in what follows unless noted otherwise.

TABLE 4: Parametrization of ϵ_S, where $\epsilon_S(R) = \alpha * \exp[-(\beta/2)(R - 3.4)]$[a]

donor/acceptor group	α	$\beta/2$ (Å^{-1})
CH_2	0.15	1.24
NH_2	0.16	1.40
PH_2	0.15	1.32
SiH_2	0.11	1.18

[a] α is equivalent to $\epsilon_S(3.4$ Å$)$.

Using SA-MCSCF wavefunction and the ϵ_C^{av} values appropriate to the SA-MCSCF connected chain from Table 3, we next considered disconnected chain results to calculate $\epsilon_S(R)$— the through-space (or van der Waals) decay constant. Because our aim is to compare with the pathways model, we present results for $\epsilon_S(R)$ directly rather than presenting H_{DA} values. In Table 4, we present the through-space decay constants for various donor/acceptor pairs, which were calculated using eq 4 (ϵ_C^{av} for N, P, and Si as D/A were 0.69, 0.65, and 0.58, respectively). The calculations of H_{DA} used to construct Table 4 were performed using eq 2 because even though the chain was broken, C_{2h} symmetry was preserved as seen in Scheme 2. All of the donor/acceptors used show very similar exponential decay ($\beta/2$ values) and values for the decay constant at 3.4 Å. Because the transferring electron is localized on the donor or the acceptor, the electron-transfer process for these systems is expected to occur via McConnell-like superexchange.[85] However, there seems to be little correlation between the energy gap between the donor/acceptor orbitals and bridge orbitals and the size of either ϵ_C or ϵ_S. [Sample values for $\Delta\epsilon_{DB}$ in fully connected chains with a total of eight atoms are 2.6 eV for CH_2 as donor, 2.85 eV for NH_2, 3.5 eV for PH_2, and 3.6 eV for SiH_2, based on UHF (C and Si) or RHF (N and P) occupied orbital energy differences. We expect these values to vary somewhat depending on whether the chain length is changed or one considers disconnected systems.]

The values of the coupling at 3.4 Å central C−C separation in Table 4 are expected to be somewhat higher than those for thermally accessible van der Waals contacts in this orientation. (MP2 calculations for two methanes oriented in the same way as the central methyl groups for this orientation show an energy rise of nearly 5 kcal/mol between 4 and 3.4 Å.) This is because the C−C line of centers connecting the central methyl carbons nearly coincides with a pair of C−H bonds. In this orientation one would generally expect a C−C distance closer to 4.2−4.4 Å[86] on the basis of the C−H bond length and H atom van der Waals radius. At a central C−C distance of 4.2 Å in this orientation the coupling elements would be decreased relative to those at 3.4 Å by a factor of approximately 0.35. We thus decided to examine other van der Waals orientations that might allow closer approach of the central methyl groups.

Table 5 presents results from another methyl−methyl orientation. In this series of calculations we examine this structure as a function of the relative orientation of the fragments. For these calculations, the plane of one of the fragments was rotated relative to the other fragment, which we characterize by the dihedral angle between the two planes as seen in Scheme 3. During these calculations the distance between the two center methyls was frozen at 3.4 Å, which is the van der Waals distance for a head-on methyl−methyl contact.[86] The donor/acceptor
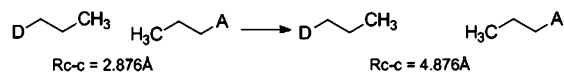
SCHEME 2: Examples of Geometries Used in the Calculations Presented in Table 4

$R_{C-C} = 2.876$ Å $R_{C-C} = 4.876$ Å

TABLE 5: H_{DA} and ϵ_S Values for the Dihedral Rotation Shown in Scheme 3

dihedral angle (deg)	H_{DA} (eV)	ϵ_S(3.4 Å)
0	0.0080	0.067
30	0.0081	0.068
60	0.0085	0.071
90	0.0089	0.075
120	0.0095	0.080
150	0.0100	0.084
180	0.0102	0.085

TABLE 6: H_{DA} and ϵ_S Values for the Rotation Illustrated in Scheme 4

twist angle (deg)	H_{DA} (eV)	ϵ_S(3.4 Å)
0	0.0102	0.085
30	0.0088	0.074
60	0.0051	0.043
90	8.00E−06	6.70E−05
120	0.0051	0.043
150	0.0088	0.074
180	0.0102	0.085

group used for any calculation should be assumed to be the CH_2 group unless otherwise noted. In Table 5, there is only a 25% change in the ϵ_S value from the largest value to the smallest value. It is perhaps surprising that the H_{DA} value is not zero when the planes of donor and acceptor are perpendicular to each other. However, because the coupling between the donor/acceptor orbitals is mediated by the bridge framework, which is not linear, the local symmetry at the donor and acceptor need not determine the overall magnitude of the electronic coupling element.

In Table 6, a second orientation effect was examined by twisting either the donor or acceptor CH_2 group independently from the rest of the molecular subunit to which it belongs, shown in Scheme 4. Here we see a "zero" H_{DA} value at 90° due to symmetry effects because a common symmetry plane occurs for both bridges at two points in the rotation. The trends seen in Table 6 are seen in the other donor/acceptor systems (results not shown).

Another degree of freedom is explored in Table 7 (see Scheme 5) in the dihedral angle between planes of the heavy atoms for each subunit, defining the angle of rotation. For these calculations, a 30° angular rotation should be equivalent to a −30° angular rotation. This rotation examines how sensitive ϵ_S is to the nearest points of contact in the van der Waals interaction. From Table 7, it is evident that small angle changes do not greatly affect the size of the electronic coupling. However, when larger angles are attained, the decay constant ϵ_S decreases by more than a factor of 3.

In Table 8, various alcohol−alcohol contacts are examined to compare several different hydrogen bond geometries and to directly compare hydrogen-bonded configurations to van der Waals contacts. In addition, we compare OH−OH H-bonds to two other H-bonded contacts (OH−NH_2 and OH−F) as well as several model van der Waals contacts. The first geometry (denoted model water dimer) was created from an optimized water dimer,[87] appending the appropriate CH_2 bridge units, and the CH_2 donor/acceptor groups. The second geometry (OH−OH B3LYP opt) was created by optimizing the starting geometry seen in Scheme 6, with R = −OH, using the B3LYP/6-31G* method. In both cases two distinct O−O distances are tested, one being the optimized distance for each structure and the other having an O−O distance at 2.8 Å (for comparison with previous calculations). The third geometry is a model hydrogen bond system equivalent to the one seen is Scheme 6 with R = −OH and the central O−O distance being 2.8 Å. The fourth geometry is a model van der Waals contact between two OH groups with the geometry being equivalent to the 180°
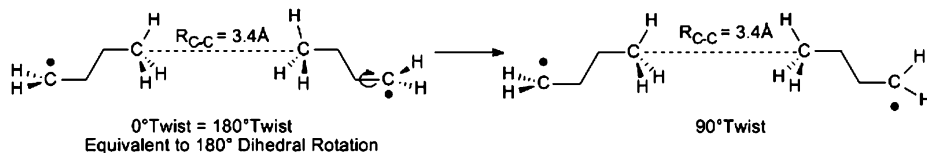
dihedral rotation seen in Scheme 3, except that the terminal bridge units are alcohols instead of methyls and the central O−O distance is 2.8 Å. A fifth geometry is chosen to explore different van der Waals contacts and was created using the 0° dihedral rotation geometry seen in Scheme 3, except that one of the bridge terminus groups is an alcohol group and the central C−O distance is 3.2 Å. The final three structures are an alcohol−amine hydrogen bond, an alcohol−fluorine hydrogen bond, and an alcohol−methyl van der Waals contact. These final three structures were all optimized structures based on use of the B3LYP/6-311++G(d,p) method. The geometries from these optimizations are very similar to the alcohol−alcohol optimized structure, except slightly more linear. Several of these structures are depicted in Figure 1. In Table 8 it is seen that there is only a small difference between the ϵ_H values and the ϵ_S values, with the ϵ_S value being larger than some of the ϵ_H values.

One might imagine that tunneling through H-bonds, which are inherently less symmetrical than methyl−methyl van der Waals contacts, might be significantly more sensitive to the relative D/A orientations. To test this we used the OH−OH B3LYP optimized structure from Table 8 with the O−O distance set equal to 2.8 Å and then rotated the donor or acceptor in 30° increments from 0° to 180°. The angle corresponding to the maximum coupling for each individual rotation was then taken to construct a dimer with (approximate) D and A orientations leading to maximal coupling. This approximate maximal coupling orientation yields a value of H_{DA} (and thus ϵ_H) approximately 1.7 times that of the value in Table 8 (ϵ_H near 0.097 rather than 0.055 as in Table 8). We performed the analogous rotation of D and A for a geometry related to this same optimized H-bond geometry, except that the two fragments were rotated relative to each other about the O−O line of centers by 180°. Here the value of ϵ_H was 0.10 before optimization of the D/A orientations and 0.19 after optimization. Thus, although such angle variations could lead to somewhat larger values of the decay constants, we would not expect drastic changes were such angle variations to be pursued in general.

In Table 9 three distinct planar hydrogen bond structures (geometries shown in Scheme 6) were examined and parametrized so that the values can be compared to the previous van der Waals results and to the results of the pathways model (CH_2 donor and acceptor). The reference distance between terminal atoms in the disconnected structure was chosen to be 2.8 Å to represent a normal hydrogen bond length. These results show that the α/ϵ_H(2.8 Å) values for the various contacts are fairly similar and are also similar to previously calculated ϵ_S values. One notable difference among these contacts is the fact that

SCHEME 3:   Diagram of the Dihedral Angle Rotations Seen in Table 5

Tunneling through Weak Interactions

J. Phys. Chem. A, Vol. 110, No. 51, 2006 **14023**
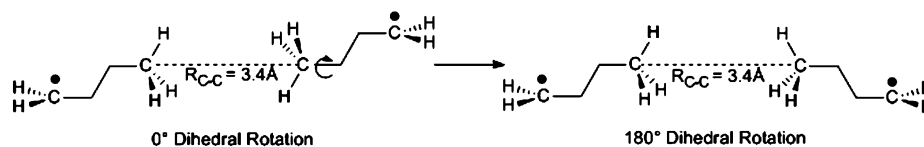
SCHEME 4: Diagram of the Donor/Acceptor Twist Examined in Table 6

0°Twist = 180°Twist
Equivalent to 180° Dihedral Rotation

90°Twist

the $\beta/2$ value for the fluorine system is larger than that for the other two systems. This could result from the fact that fluorine is very electronegative, which will cause the electron density to be locally compact, leading to a greater sensitivity to the separation distance. Whereas at large separation the decay with distance of H_{DA} will be controlled by the energy of the donor and acceptor, the local structure of the electron density clearly also plays a role for small variations in distance.

Table 10 demonstrates the differences in ϵ_H values based on the choice of donor/acceptor groups. For all of these systems, an alcohol−alcohol hydrogen bond system at 2.8 Å was used as the reference distance and the orientation was the same as that of Scheme 6. There is modest sensitivity to the D/A choice, on a scale comparable to the sensitivity found for van der Waals contacts (Table 4).

In Table 11, the effects of increasing the size of the basis set on two disconnected chain geometries are examined. The first geometry is similar to the OH−OH hydrogen bond from Table 8 based on the model water dimer geometry presented there, but rotated around the O−O line of centers (yielding a somewhat greater coupling element than that quoted for the model water dimer structure). The second geometry is the van der Waals structure at the 120° angle of Table 5. The previous results for these geometries using the 6-31G* basis are presented again in Table 11, along with results from systematic expansion of the basis up to the 6-311++G(d,p) basis set. Because all of the results presented are within about 15% of the 6-31G* results, we believe that the 6-31G* basis was sufficiently accurate for our purposes.

Using a variety of systems, Table 12 examines the effect on the electronic coupling of including correlation via the EOM-CCSD method. The variation in the coupling between correlated and uncorrelated results is at most 25%. Results for other geometries (not shown) tell a similar story—a maximum change in the coupling of about 33%. Thus, the uncorrelated SA-MCSCF method appears to be sufficiently accurate for the present treatment and, at least in cases examined here, correlation does not have a large impact on the H_{DA} value for these systems.

We also applied FOCI and SOCI wavefunctions to model CH_3-CH_3 van der Waals geometries. The largest variation in the coupling compared to the SA-MCSCF results was a factor of 1.5. We again concluded that correlation had at most a quantitative effect on the coupling and that the conclusions we draw would not be altered by the inclusion of correlation.

4. Discussion

The pathways model has been used extensively as a conceptual and computational point of reference for understanding

biological electron transfers. From a conceptual point of view its main elements are that (i) through-bond coupling decays slowly, (ii) tunneling through weak interactions decays quite rapidly, and (iii) H-bonds, although they are relatively weak interactions, still mediate the electronic coupling quite effectively. For comparison with our calculated results we note the pathways model values for $\epsilon_C = 0.6$, $\epsilon_S(3.4\text{ Å}) = 0.010$, and $\epsilon_H(2.8\text{ Å}) = 0.36$ (the two distances being the van der Waals distances for head-on contact for methyl groups and a conventional H-bond length, respectively).[21,70]

In a general sense, our results support the pathways model. The through-bond decay constant for the connected alkane chains is quite similar to that of the pathways model, is weakly dependent on the donor or acceptor, and is considerably larger than the decay constant for tunneling through weak interactions. Clearly the through-bond coupling will vary with geometry, and our results are focused solely on all-trans geometries. However, the variation is not expected to qualitatively alter these conclusions. Our results support the notion that electrons or holes should tunnel through-bond whenever the path connecting D and A is not too circuitous.

We find considerable variation in the decay constants for H-bond and van der Waals contacts as a function of geometry, making it difficult to be absolutely general about the relative strengths of the two types of interactions. We observe, for the range of geometries considered here, that decay constants for either type of interaction are generally below 0.1 (for the reference distances considered) but above 0.03. Considering only the largest interactions of each type, we obtained an H-bond decay constant of nearly 0.2, with a thermally accessible van der Waals decay constant of at most 0.085. This would argue that the H-bonded contacts have the potential to produce couplings larger than the van der Waals contacts. However, taken in aggregate our results indicate that, if there are differences on average between the two types of weak-coupling-mediated tunneling, they are modest at best. Recent work by Prytkova, Kurnikov, and Beratan has also posited a somewhat greater size for through-space coupling than in the original pathways model.[88] Their results suggest better agreement for the pathways model with ab initio data when they decrease the through-space decay constant from 1.7 to 1.0 Å^{-1}. In their case the decreased decay constant size was in part accounted for by the assumption of tunneling at elevated energies via excited states. In the present cases we are considering tunneling for low-energy electrons and still find larger than expected through-space tunneling.

Of course, the question of the relative size of the through-bond and through-space/H-bond coupling is in part dependent on how one calculates the through-space coupling, and there is some ambiguity associated with the optimal method for doing this. For example, consider the value of ϵ_S (derived from Table 4) for symmetrical van der Waals contacts at 3.4 Å for D/A = CH_2, 0.145. The value of ϵ_C used to obtain this (and all values of ϵ_S and ϵ_H in the rest of the paper) was the average value from Table 3, that is, $\epsilon_C = 0.64$. One might have imagined that a better choice would have been that appropriate to the $n = 10$ (connected chain) result, $\epsilon_C = 0.588$, because the connected

TABLE 7: H_{DA} and ϵ_S Values for the Rotation Shown in Scheme 5

angular rotation (deg)	H_{DA} (eV)	ϵ_S(3.4 Å)
90	0.0035	0.029
60	0.0024	0.020
30	0.0066	0.055
0	0.0080	0.067
−30	0.0066	0.055

SCHEME 5: (Top) Axis of Rotation for the Angular Rotation Calculation in Table 7; (Bottom) Top View of Two Angular Rotation Geometries
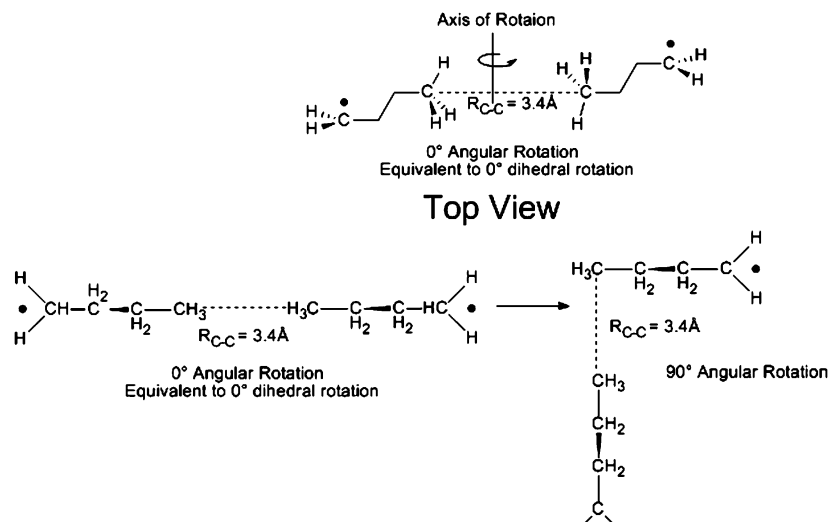
and disconnected systems used to derive the results of Table 3 were based on $n = 10$ systems. In this case, $\epsilon_S(3.4$ Å$) = 0.112$ (based on the connected H_{DA} value of 0.0313 eV for the $n = 10$ case and the disconnected H_{DA} value of 0.0173 eV). A third, distinct method for calculating ϵ_S would be to use $\epsilon_C = 0.74$ (for the $n = 4/6$) for the disconnected chain (because there are two distinct $n = 4$ chains in the $n = 10$ disconnected chain results), whereas for the connected $n = 10$ chain $\epsilon_C = 0.588$ would be used (see eq 5).

$$\frac{H_{DA}^{disconnected,n=10}}{H_{DA}^{connected,n=10}} \frac{(\epsilon_C^{n=10/12})^8}{(\epsilon_C^{n=4/6})^5} = \epsilon_S(3.4\text{Å}) \qquad (5)$$

Using eq 5 we find that $\epsilon_S(3.4$ Å$) = 0.036$, a significant difference compared to the previous two estimates. To assess the validity of this result, we performed calculations based on the $n = 12$ and $n = 14$ connected and disconnected chains. If variation in ϵ_C is an issue (necessitating use of eq 5), then ϵ_S should vary significantly when eq 5 is used to calculate ϵ_S on the basis of the $n = 12$ and $n = 14$ systems. As Table 13 demonstrates, the $\epsilon_S(3.4$ Å$)$ value based on the $n = 10$ system is actually lower than the $\epsilon_S(3.4$ Å$)$ value for either the $n = 12$

TABLE 8: Comparison of Various Alcohol–Alcohol and Hydrogen Bond Contacts[a]

structure	contact	H_{DA} (eV)	ϵ_H or ϵ_S	distance between heavy atoms (Å)
model water dimer	H-bond	0.00244	0.020	2.8
model water dimer	H-bond	0.00223	0.019	2.91
OH–OH/B3LYP opt	H-bond	0.00673	0.055	2.8
OH–OH/B3LYP opt	H-bond	0.00649	0.054	2.85
model H-bond	H-bond	0.0117	0.098	2.8
OH–OH VDW contact	VDW	0.00847	0.071	2.8
model VDW OH–CH$_3$	VDW	0.00710	0.059	3.2
opt OH–NH$_2$	H-bond	0.00633	0.053	2.90
opt OH–F	H-bond	0.00599	0.050	2.91
opt OH–CH$_3$	VDW	0.00153	0.013	3.1

[a] Contact indicates the qualitative character of the interaction between the two central units on the pair of disconnected chains. The origin of the specific geometries is outlined in the text. The final column indicates the distance between the pair of central heavy atoms.

or 14 system. Thus, we expect that at worst our ϵ_S values underestimate what we would obtain for longer systems and that the conclusions drawn here about the relative sizes of these interactions should be relatively robust. Furthermore, because the same analysis is used to compute ϵ_H and ϵ_S, these two quantities can be directly compared, independent of how one might prefer to derive either one by itself.
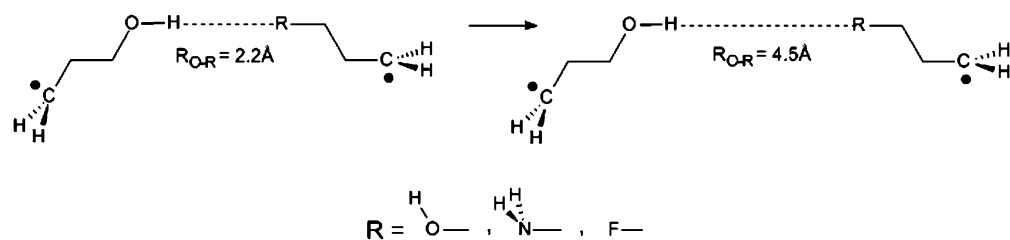
A second issue to consider in comparing coupling through H-bonds and van der Waals contacts is the distance between heavy atoms in the van der Waals contact. In the present study our H-bond reference distances are near 2.8 Å, and we have chosen a reference value of 3.4 Å for methyl–methyl van der Waals contact. This value for methyl–methyl van der Waals contacts allows direct comparison with previous calculations[30] and is in agreement with the expected C–C distance for head-on approach of two methyl groups.[86] However, whereas H-bonds have generally well-defined lengths, van der Waals contacts range over considerable lengths and will often depend on how a protein folds. Their lengths will also likely be more susceptible to thermal fluctuations than H-bonds. Methyl–methyl van der Waals contacts have been observed in the range of 3.4–4.2 Å in crystal structures of organic molecules.[86] In a crystal structure of cytochrome c a C–C distance of 3.22 Å is found between an isoleucine and leucine (residues 85 and 94),[89] but there are certainly larger van der Waals contact distances observed as well. An increase in distance from 3.4 to 4.0 Å would decrease our ϵ_S values by approximately a factor of 2 (on the basis of the exponential distance dependence presented in Table 3), which is still a considerably larger coupling than the factor of 36 decrease for through-space coupling relative to H-bonds in the pathways model. Thus, if one compared "normal" length H-bonds to stretched van der Waals contacts, coupling through H-bonds would be, on average, about a factor of 2 larger. However, if one compares tunneling through each type of contact at near-optimal lengths for the interaction, the tunneling decay parameters are relatively similar. Finally, we note that if we were to compare the two types of contacts at a single fixed distance (e.g., 2.8 Å), we expect that tunneling through van der Waals contacts would be at least as efficient as tunneling through H-bonds, because the methyl groups would be quite close and in a relatively high potential energy configuration. This is, however, a relatively unlikely geometry for van der Waals contacts, and we have not considered it here.

Tunneling through Weak Interactions

J. Phys. Chem. A, Vol. 110, No. 51, 2006 **14025**

SCHEME 6: Diagram of the Generalized Structures Used To Calculate the Values in Tables 8 and 9

As suggested in the analysis that led to the pathways model, we find considerable orientation dependence in the coupling through the weak interactions considered here. The couplings via different van der Waals orientations examined in Tables 5−7 show significant variation with geometry, and it is clear from the consideration of H-bonds that small geometry changes can lead to large changes in the coupling. The pathways model treats these orientation effects in an average sense, and they are indeed non-negligible.

One might ask how sensitive the present results are to D/A energy variations. The energies of the transferring electron relative to the bridge HOMO vary over a range of about 2.5−4 eV in the present examples. For photoexcited electron transfer one would expect a larger D/A bridge gap and a smaller D/A IP. The present results cannot directly comment on these larger gap situations; however, past results for tunneling through water, for both H-bonded and non-H-bonded configurations, suggest relatively modest variations in the coupling at close contact for significantly larger changes in D/A bridge energies.[57,58] We expect similar behavior for these systems, and this is consistent with the relatively weak dependence of tunneling through bond on D/A energy when the D/A energies are well-separated from the bridge band edges.[90] Nonetheless, we still expect the D/A energy to affect the exponential decay constant for the coupling at large distances. In addition, it is interesting to note that the decay with distance is affected (locally) by the nature of the central contacts, with H-bond-mediated tunneling through F decaying more rapidly with distance than tunneling through methyl groups. At large distances this decay should depend largely on the D/A energy, but it is clear that at shorter distances the decay depends to some extent on the features of the local electron density.

The central, and somewhat surprising, result of the present work is the similarity between the coupling through-space (van der Waals contacts) and that through H-bonds. As noted above, the pathways model (on the basis of a pair of simple analytical models) suggested that the difference in the size of these couplings should be a factor of about 36 (at distances of 3.4 and 2.8 Å for through-space- and H-bond-mediated coupling, respectively). Despite the relatively large orientation dependence observed in our results, we find H-bond-mediated coupling to be a good deal weaker and through-space coupling to be a good deal stronger than these predictions. In some sense this should not be too surprising, because we are comparing tunneling

efficiencies through two weak interactions and there is little reason to assume that the efficiency of tunneling should necessarily scale with the strength of interactions at these low energies.

It is possible that this result is specific to the systems studied here. However, the robust nature of the result with respect to D/A energy and orientation suggests that it may be relatively general. One might also suggest that the basis and SA-MCSCF treatment used here are inadequate for uncovering the difference between the two types of tunneling, but our extended basis set and correlation results (as seen in Tables 11 and 12) do not show dramatic changes in the coupling.

If these results are general, they suggest that *for fixed geometries* there are really only two types of coupling—bond-mediated and weak-interaction-mediated, with bond-mediated coupling being at least 6 times slower decaying (i.e., one weak-interaction tunneling event is equivalent to tunneling through at least four covalent bonds, and often more like five or six covalent bonds). If that is true, what might account for previous suggestions that H-bonds are significantly more effective at mediating coupling than van der Waals contacts?[8,23,91]

One possibility is that the comparisons between H-bonded and covalently mediated couplings have been made for covalent structures that possess interference effects and/or poor coupling to the donor or acceptor due to stearic effects.[23] Subtle geometry changes not accounted for by counting bonds may play a role that could mask weaker coupling by H-bonds. We are pursuing calculations to test this, but the present results do not support suggestions of particularly robust coupling through single H-bonds.

It is also possible that H-bonds might be found to be more effective at mediating coupling than van der Waals contacts than our results indicate due to a secondary effect. That is, the strengths of the couplings through van der Waals and H-bonds might be quite similar, but the H-bond's strength might confer extra stability to the overall structure with respect to geometrical fluctuations. It is well-known now that small fluctuations can yield rapid and often dramatic changes in the coupling.[57,92−95] It is possible that the reason H-bonds may be better contacts, if indeed they are, is due to the extra stability of the structure when H-bonds are present rather than absent, giving rise to smaller coupling fluctuations and (if the geometry near the minimum corresponds to relatively large coupling) an overall rate enhancement.
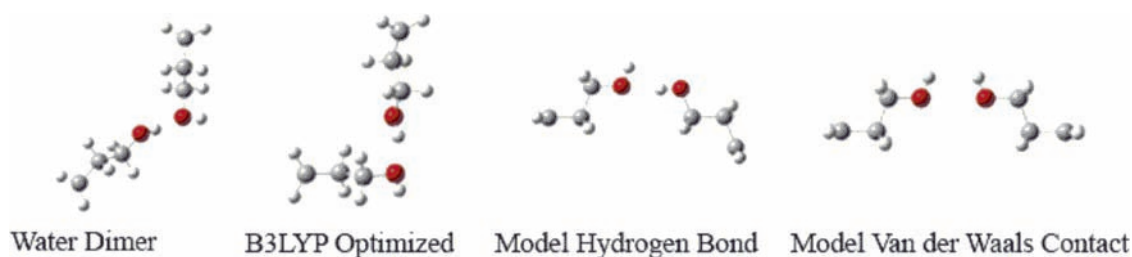

Figure 1. Subset of the structures considered in the calculations presented in Table 8.

TABLE 9: Parametrization of ϵ_H, where $\epsilon_H(R) = \alpha *$ $\exp[-(\beta/2)(R - 2.8)]^a$

hydrogen bond group	$\epsilon_H(2.8$ Å$)$	$\beta/2$ (Å^{-1})
OH−H	0.098	1.48
OH−F	0.079	1.71
OH−NH$_2$	0.116	1.44

^{a} α is equivalent to $\epsilon_H(2.8$ Å$)$.

TABLE 10: ϵ_H Values for Various Donor/Acceptor Groups Based on the Model H-Bond Geometry

donor/acceptor group	$\epsilon_H(2.8$ Å$)$
CH$_2$	0.098
NH$_2$	0.061
SiH$_2$	0.099
PH$_2$	0.077

TABLE 11: H_{DA} (eV) Values Based on SA-MCSCF Wavefunctions for Two Geometries for a Variety of Basis Sets

system type	6-31G*	6-31++G*	6-311G(d,p)	6-311G++(d,p)
hydrogen bond	0.00908	0.00926	0.00945	0.00769
van der Waals	0.00950	0.00959	0.00963	0.00946

TABLE 12: H_{DA} (eV) Values for Several Geometries Using Correlated and Noncorrelated Methods

system type	Table^a	EOM-CCSD/ 6-31G*	SA-MCSCF/ 6-31G*
OH−OH VDW contact	8	0.00935	0.00847
methyl−methyl VDW	5 (120°)	0.0119	0.0095
methyl−methyl VDW	5 (180°)	0.0128	0.0102
OH−OH model H-bond	8	0.0118	0.0117

^{a} Indicates where this geometry was considered previously in the present study.

TABLE 13: Variation in ϵ_S Based on SA-MCSCF Results for Various n Length Systems

n	connected H_{DA} (eV)	disconnected H_{DA} (eV)	$\epsilon_S(3.4$ Å$)$	ϵ_C
10	0.0313	0.0173	0.112	0.588
12	0.0114	0.00814	0.157	0.604
14	0.00417	0.00287	0.152	0.604

Of course, to investigate detailed questions concerning the electronic coupling in systems of biological interest, one will need to go beyond coarse-grained models of the pathways type to probe subtle, specific coupling enhancements with changes in local structure. These calculations have been pursued in a number of groups with great success.[34−36,42,96−102] We have recently implemented a one-electron version of the generalized Mulliken−Hush approach[103,104] (Koopmans' theorem GMH, along with a density functional theory-based variant, Kohn−Sham GMH/KS-GMH) that will allow us to calculate couplings in systems of the appropriate scale for biological electron transfers. Thus, we are not advocating that with improved parameters one could eschew detailed calculations and obtain accurate results.

Rather, we are arguing that in thinking about the paths through which electrons might tunnel in biological (or synthetic) electron-transfer systems, it may be important to reconsider the roles of both through-space and H-bond tunneling. In particular, for close van der Waals contacts tunneling may be equally effective as that through H-bonds, and a good deal larger than has been previously supposed. In addition, when considering tunneling through particular H-bonds, it may in fact be the case that the intrinsic tunneling is not significantly larger than that through other weak interactions and that the overall net tunneling comes about through the participation of a broader array of

contributions from many weak interactions. Whatever the case, the present study suggests that a new consideration of weak interactions in biological electron transfers be undertaken, using detailed, many-electron approaches, and specific focus be given to tunneling through weak interactions. The tunneling current approach of Stuchebruhkov[2,3,105] and co-workers appears to be ideally suited to address this question in realistic systems.

5. Conclusions

We presented results from ab initio electronic structure theory calculations on model systems that allow detailed comparisons of tunneling through bonded contacts, H-bonds, and van der Waals contacts. Considerable geometrical sensitivity as well as an exponential distance dependence of the tunneling is observed for tunneling through nonbonded contacts. However, the fundamental result from the present study is that we find at best modest differences between tunneling mediated by H-bonds and tunneling mediated by van der Waals contacts at conventional distances for each interaction. We suggest that this may imply that van der Waals contacts may be more important in biological electron transfers than has been previously assumed and that the focus on specific H-bonds that mediate interchain tunneling may exaggerate their importance. However, we also discuss a possible secondary role H-bonds may play in controlling geometrical fluctuations that can give rise to increased tunneling.

References and Notes

(1) Marcus, R. A.; Sutin, N. *Biochim. Biophys. Acta* **1985**, *811*, 265.
(2) Stuchebrukhov, A. A. *J. Chem. Phys.* **1996**, *105* (24), 10819−10829.
(3) Stuchebrukhov, A. A. *J. Chem. Phys.* **1996**, *104* (21), 8424−8432.
(4) Stuchebrukhov, A. A. *J. Chem. Phys.* **1998**, *108* (20), 8499−8509.
(5) Gray, H. B. *Proc. Natl. Acad. Sci. U.S.A.* **2003**, *100* (7), 3563−3568.
(6) Gray, H. B.; Malmstrom, B. G. *Biochemistry* **1989**, *28* (19), 7499−7505.
(7) Gray, H. B.; Winkler, J. R. *Annu. Rev. Biochem.* **1996**, *65*, 537.
(8) Gray, H. B.; Winkler, J. R. *Proc. Natl. Acad. Sci. U.S.A.* **2005**, *102* (10), 3534−3539.
(9) Skourtis, S. S.; Beratan, D. N. Theories of structure−function relationships for bridge-mediated electron transfer reactions. *Electron Transfer: Isol. Mol. Biomol., Part 1* **1999**, *106*, 377−452.
(10) DeVault, D. *Quantum Mechanical Tunneling in Biological Systems*, 2nd ed.; Cambridge University Press: New York, 1984.
(11) Marcus, R. A. *J. Chem. Phys.* **1965**, *43*, 679.
(12) Hush, N. S. *Trans. Faraday Soc.* **1961**, *57*, 557.
(13) Levich, V. G. *Adv. Electrochem. Electrochem. Eng.* **1966**, *4*, 249.
(14) Dogonadze, R. R.; Kuznetsov, A. M.; Vorotyntsev. *Phys. Status Solidi B* **1972**, *54*, 125, 425.
(15) Kestner, N. R.; Logan, J.; Jortner, J. *J. Phys. Chem.* **1974**, *78*, 2148.
(16) Bixon, M.; Jortner, J. Electron transfer−from isolated molecules to biomolecules. *Electron Transfer: Isol. Mol. Biomol., Part 1* **1999**, *106*, 35−202.
(17) Newton, M. D.; Sutin, N. *Annu. Rev. Phys. Chem.* **1985**, *35*, 437.
(18) Skourtis, S. S.; Onuchic, J. N.; Beratan, D. N. *Inorg. Chim. Acta* **1996**, *243* (1−2), 167−175.
(19) Onuchic, J. N.; Beratan, D. N. *J. Chem. Phys.* **1990**, *92*, 722.
(20) Beratan, D. N.; Onuchic, J. N. *Adv. Chem. Ser.* **1991**, *No. 228*, 71−90.
(21) Onuchic, J. N.; Beratan, D. N.; Winkler, J. R.; Gray, H. B. *Annu. Rev. Biophys. Biomol. Struct.* **1992**, *21*, 349−377.
(22) Casimiro, D. R.; Beratan, D. N.; Onuchic, J. N.; Winkler, J. R.; Gray, H. B. Donor−acceptor electronic coupling in ruthenium-modified heme proteins. *Mech. Bioinorg. Chem.* **1995**, *246*, 471−485.
(23) Rege, P. J.; Williams, S. A.; Therien, M. J. *Science* **1995**, *269*, 1409.
(24) Onuchic, J. N.; Beratan, D. N.; Winkler, J. R.; Gray, H. B. *Annu. Rev. Biophys. Biomol. Struct.* **1992**, *21*, 349.

Tunneling through Weak Interactions

J. Phys. Chem. A, Vol. 110, No. 51, 2006 **14027**

(25) Onuchic, J. N.; Beratan, D. N. *J. Chem. Phys.* **1990**, *92* (1), 722−733.

(26) Curtiss, L. A.; Miller, J. R. *J. Phys. Chem. A* **1998**, *102*, 160−167.

(27) Curtiss, L. A.; Naleway, C. A.; Miller, J. R. *J. Phys. Chem.* **1993**, *97*, 4050.

(28) Curtiss, L. A.; Naleway, C. A.; Miller, J. R. *J. Phys. Chem.* **1995**, *99*, 1182−1193.

(29) Liang, C.; Newton, M. D. *J. Phys. Chem.* **1992**, *96*, 2855.

(30) Liang, C.; Newton, M. D. *J. Phys. Chem.* **1992**, *97*, 3199.

(31) Stuchebrukhov, A. A. *Int. J. Quantum Chem.* **2000**, *77* (1), 16−26.

(32) Stuchebrukhov, A. A. Toward ab initio theory of long-distance electron tunneling in proteins: tunneling currents approach. *Adv. Chem. Phys.* **2001**, *118*, 1−44.

(33) Stuchebrukhov, A. A. *Theor. Chem. Acc.* **2003**, *110* (5), 291−306.

(34) Kurnikov, I. V.; Beratan, D. N. *Abstr. Pap. Am. Chem. Soc.* **1995**, *210*, 119-INOR.

(35) Kurnikov, I. V.; Beratan, D. N. *J. Chem. Phys.* **1996**, *105* (21), 9561−9573.

(36) Kurnikov, I. V.; Beratan, D. N. *Biophys. J.* **2001**, *80* (1), 186.

(37) Larsson, S.; Braga, M. *J. Photochem. Photobiol. A: Chem.* **1994**, *82* (1−3), 61−66.

(38) Larsson, S.; Broo, A.; Sjolin, L. *J. Phys. Chem.* **1995**, *99*, 4860−4865.

(39) Larsson, S.; Klimkans, A. *J. Mol. Struct.−THEOCHEM* **1999**, *464* (1−3), 59−65.

(40) Larsson, S.; RodriguezMonge, L. *Int. J. Quantum Chem.* **1996**, *58* (5), 517−532.

(41) Hsu, C. P.; Marcus, R. A. *J. Chem. Phys.* **1997**, *106* (2), 584−598.

(42) Gehlen, J. N.; Daizadeh, I.; Stuchebrukhov, A. A.; Marcus, R. A. *Inorg. Chim. Acta* **1996**, *243* (1−2), 271−282.

(43) Lee, M. K.; Shephard, M. J.; Risser, S. M.; Priyadarshy, S.; Paddon-Row, M. N.; Beratan, D. N. *J. Phys. Chem. A* **2000**, *104*, 7593−7599.

(44) Shephard, M. J.; Paddon-Row, M. N.; Jordan, K. D. *J. Am. Chem. Soc.* **1994**, *116*, 5328.

(45) Jordan, K. D.; Nachtigallova, D.; Paddon-Row, M. N. Long-range intramolecular interactions: implications for electron transfer. In *Modern Electronic Structure Theory and Applications in Organic Chemistry*; Davidson, E. R., Ed.; World Science: Hackensack, NJ, 1997; p 257.

(46) Miller, J. R.; Beitz, J. V.; Huddleston, R. K. *J. Am. Chem. Soc.* **1984**, *106*, 5057−5068.

(47) Miller, J. R.; Beitz, J. V. *J. Chem. Phys.* **1981**, *74* (12), 6746−6756.

(48) Beitz, J. V.; Miller, J. R. *J. Chem. Phys.* **1979**, *71* (11), 4579−4595.

(49) Wenger, O. S.; Leigh, B. S.; Villahermosa, R. M.; Gray, H. B.; Winkler, J. R. *Science* **2005**, *307* (5706), 99−102.

(50) Ponce, A.; Gray, H. B.; Winkler, J. R. *J. Am. Chem. Soc.* **2000**, *122*, 8187−8191.

(51) Cave, R. J.; Newton, M. D.; Kumar, K.; Zimmt, M. B. *J. Phys. Chem.* **1995**, *99*, 17501−17504.

(52) Kumar, K.; Kurnikov, I. V.; Beratan, D. N.; Waldeck, D. H.; Zimmt, M. B. *J. Phys. Chem. A* **1998**, *102*, 5529−5541.

(53) Kaplan, R. W.; Napper, A. M.; Waldeck, D. H.; Zimmt, M. B. *J. Am. Chem. Soc.* **2000**, *122*, 12039−12040.

(54) Zimmt, M. B.; Waldeck, A. H. *J. Phys. Chem. A* **2003**, *107*, 3580−3597.

(55) Napper, A. M.; Read, I.; Waldeck, D. H.; Head, N. J.; Oliver, A. M.; Paddon-Row, M. N. *J. Am. Chem. Soc.* **2000**, *122*, 5220.

(56) Newton, M. D. *J. Electroanal. Chem.* **1997**, *438* (1−2), 3−10.

(57) Miller, N. E.; Wander, M. C.; Cave, R. J. *J. Phys. Chem. A* **1999**, *103*, 1084−1093.

(58) Cukier, E.; Daniels, S.; Vinson, E.; Cave, R. J. *J. Phys. Chem. A* **2002**, *106*, 11240−11247.

(59) Tezcan, F. A.; Crane, B. R.; Winkler, J. R.; Gray, H. B. *Proc. Natl. Acad. Sci. U.S.A.* **2001**, *98*, 5002.

(60) Dennington II, R. K. T.; Millam, J.; Eppinnett, K.; Hovell, W. L.; Gilliland, R. *Gaussview* 3.09; Semichem, Inc.: Shawnee Mission, KS, 2003.

(61) Koch, W.; Holthausen, M. C. *A Chemist's Guide to Density Functional Theory*, 2nd ed.; Wliey-VCH: New York, 2001.

(62) Becke, A. D. *J. Chem. Phys.* **1993**, *98*, 5648−5652.

(63) Rassolov, V. A.; Ratner, M. A.; Pople, J. A.; Redfern, P. C.; Curtiss, L. A. *J. Comput. Chem.* **2001**, *22* (9), 976−984.

(64) Curtiss, L. A.; McGrath, M. P.; Blaudeau, J. P.; Davis, N. E.; Binning, R. C.; Radom, L. *J. Chem. Phys.* **1995**, *103* (14), 6104−6113.

(65) Gordon, M. S. *Chem. Phys. Lett.* **1980**, *76* (1), 163−168.

(66) Harihara, P. C.; Pople, J. A. *Mol. Phys.* **1974**, *27* (1), 209−214.

(67) Harihara, P. C.; Pople, J. A. *Theor. Chim. Acta* **1973**, *28* (3), 213−222.

(68) Hehre, W. J.; Ditchfie, R.; Pople, J. A. *J. Chem. Phys.* **1972**, *56* (5), 2257.

(69) Ditchfie, R.; Hehre, W. J.; Pople, J. A. *J. Chem. Phys.* **1971**, *54* (2), 724.

(70) Cukier, E.; Cave, R. J. *Chem. Phys. Lett.* **2005**, *402*, 186−191.

(71) Mulliken, R. S. *J. Am. Chem. Soc.* **1952**, *64*, 811.

(72) Hush, N. S. *Electrochim. Acta* **1968**, *13*, 1005.

(73) Cave, R. J.; Newton, M. D. *Chem. Phys. Lett.* **1996**, *249* (1−2), 15−19.

(74) Cave, R. J.; Newton, M. D. *J. Chem. Phys.* **1997**, *106* (22), 9213−9226.

(75) Stanton, J. F.; Bartlett, R. J. *J. Chem. Phys.* **1993**, *98*, 7029.

(76) Szabo, A.; Ostlund, N. S. *Modern Quantum Chemistry: Introduction to Advanced Electronic Structure Theory*, 2nd ed.; MacMillan: New York, 1982.

(77) Frisch, M. J.; Trucks, G. W.; Schlegel, H. B.; Scuseria, G. E.; Robb, M. A.; Cheeseman, J. R.; Zakrzewski, V. G.; Montgomery, J. A., J.; Stratmann, R. E.; Burant, J. C.; Dapprich, S.; Millam, J. M.; Daniels, A. D.; Kudin, K. N.; Strain, M. C.; Farkas, O.; Tomasi, J.; Barone, V.; Cossi, M.; Cammi, R.; Mennucci, B.; Pomelli, C.; Adamo, C.; Clifford, S.; Ochterski, J.; Petersson, G. A.; Ayala, P. Y.; Cui, Q.; Morokuma, K.; Salvador, P.; Dannenberg, J. J.; Malick, D. K.; Rabuck, A. D.; Raghavachari, K.; Foresman, J. B.; Cioslowski, J.; Ortiz, J. V.; Baboul, A. G.; Stefanov, B. B.; Liu, G.; Liashenko, A.; Piskorz, P.; Komaromi, I.; Gomperts, R.; Martin, R. L.; Fox, D. J.; Keith, T.; Al-Laham, M. A.; Peng, C. Y.; Nanayakkara, A.; Challacombe, M.; Gill, P. M. W.; Johnson, B.; Chen, W.; Wong, M. W.; Andres, J. L.; Gonzalez, C.; Head-Gordon, M.; Replogle, E. S.; Pople, J. A. *Gaussian 98*, revision A.11.3; Gaussian, Inc.: Pittsburgh, PA, 2001.

(78) Frisch, M. J. T. G. W.; Schlegel, H. B.; Scuseria, G. E.; Robb, M. A.; Cheeseman, J. R.; Montgomery, J. A., Jr.; Vreven, T.; Kudin, K. N.; Burant, J. C.; Millam, J. M.; Iyengar, S. S.; Tomasi, J.; Barone, V.; Mennucci, B.; Cossi, M.; Scalmani, G.; Rega, N.; Petersson, G. A.; Nakatsuji, H.; Hada, M.; Ehara, M.; Toyota, K.; Fukuda, R.; Hasegawa, J.; Ishida, M.; Nakajima, T.; Honda, Y.; Kitao, O.; Nakai, H.; Klene, M.; Li, X.; Knox, J. E.; Hratchian, H. P.; Cross, J. B.; Bakken, V.; Adamo, C.; Jaramillo, J.; Gomperts, R.; Stratmann, R. E.; Yazyev, O.; Austin, A. J.; Cammi, R.; Pomelli, C.; Ochterski, J. W.; Ayala, P. Y.; Morokuma, K.; Voth, G. A.; Salvador, P.; Dannenberg, J. J.; Zakrzewski, V. G.; Dapprich, S.; Daniels, A. D.; Strain, M. C.; Farkas, O.; Malick, D. K.; Rabuck, A. D.; Raghavachari, K.; Foresman, J. B.; Ortiz, J. V.; Cui, Q.; Baboul, A. G.; Clifford, S.; Cioslowski, J.; Stefanov, B. B.; Liu, G.; Liashenko, A.; Piskorz, P.; Komaromi, I.; Martin, R. L.; Fox, D. J.; Keith, T.; Al-Laham, M. A.; Peng, C. Y.; Nanayakkara, A.; Challacombe, M.; Gill, P. M. W.; Johnson, B.; Chen, W.; Wong, M. W.; Gonzalez, C.; Pople, J. A. *Gaussian 03*; Gaussian Inc.: Wallingford, CT, 2004.

(79) Schmidt, M. W. B.; K. K.; Boatz, J. A.; Elbert, S. T.; Gordon, M. S.; Jensen, J. H. K., S.; Matsunaga, N.; Nguyen, K. A.; Su, S.; Windus, T. L.; Dupuis, M. M., J. A. *J. Comput. Chem.* **1993**, *14*, 1347−1363.

(80) Stanton, J. F.; Gauss, J.; Watts, J. D.; Nooijen, M.; Oliphant, N.; Perera, S. A.; Szalay, P. G.; Lauderdale, W. J.; Kucharski, S. A.; Gwaltney, S. R.; Beck, S.; Balková, A.; Bernholdt, D. E.; Baeck, K. K.; Rozyczko, P.; Sekino, H.; Hober, C.; Bartlett, R. J. *Aces II*; Quantum Theory Project: Gainesville, FL, 1999.

(81) Frisch, M. J.; Pople, J. A.; Binkley, J. S. *J. Chem. Phys.* **1984**, *80* (7), 3265−3269.

(82) Clark, T.; Chandrasekhar, J.; Spitznagel, G. W.; Schleyer, P. V. *J. Comput. Chem.* **1983**, *4* (3), 294−301.

(83) McLean, A. D.; Chandler, G. S. *J. Chem. Phys.* **1980**, *72* (10), 5639−5648.

(84) Krishnan, R.; Binkley, J. S.; Seeger, R.; Pople, J. A. *J. Chem. Phys.* **1980**, *72* (1), 650−654.

(85) McConnell, H. M. *J. Chem. Phys.* **1961**, *35*, 508.

(86) Bondi, A. *J. Phys. Chem.* **1964**, *68*, 441−451.

(87) Feller, D. *J. Chem. Phys.* **1992**, *96*, 6104.

(88) Prytkova, T. R.; Kurnikov, I. V.; Beratan, D. N. *J. Phys. Chem. B* **2005**, *109*, 1618−1625.

(89) Bushnell, G. W.; Louie, G. V.; Brayer, G. D. *J. Mol. Biol.* **1990**, *214* (2), 585−595.

(90) Beratan, D. N. *J. Am. Chem. Soc.* **1986**, *108*, 4321−4326.

(91) Yang, J.; Seneviratne, D.; Arbatin, G.; Andersson, A. M.; Curtis, J. C. *J. Am. Chem. Soc.* **1997**, *119*, 5329.

(92) Daizadeh, I.; Medvedev, E. S.; Stuchebrukhov, A. A. *Proc. Natl. Acad. Sci. U.S.A.* **1997**, *94* (8), 3703−3708.

(93) Castner, E. W.; Kennedy, D.; Cave, R. J. *J. Phys. Chem. A* **2000**, *104*, 2869−2885.

(94) Skourtis, S. S.; Balabin, I. A.; Kawatsu, T.; Beratan, D. N. *Proc. Natl. Acad. Sci. U.S.A.* **2005**, *102* (10), 3552−3557.

(95) Balabin, I. A.; Onuchic, J. N. *Science* **2000**, *290*, 114−117.

(96) Kurnikov, I. V.; Charnley, A. K.; Beratan, D. N. *J. Phys. Chem. B* **2001**, *105*, 5359−5367.

(97) Kurnikov, I. V.; Tong, G. S. M.; Madrid, M.; Beratan, D. N. *J. Phys. Chem. B* **2002**, *106*, 7−10.

(98) Kuznetsov, A. M.; Ulstrup, J. *Bioelectrochem. Bioenerg.* **1989**, *21* (3), 289−305.

(99) Daizadeh, I.; Medvedev, D. M.; Stuchebrukhov, A. A. *Mol. Biol. Evol.* **2002**, *19* (4), 406−415.

(100) Stuchebrukhov, A. *J. Inorg. Biochem.* **2001**, *86* (1), 101−101.

(101) Kim, J.; Stuchebrukhov, A. *J. Phys. Chem. B* **2000**, *104*, 8606−8613.

(102) Cheung, M. S.; Daizadeh, I.; Stuchebrukhov, A. A.; Heelis, P. F. *Biophys. J.* **1999**, *76* (3), 1241−1249.

(103) Voityuk, A. A.; Rosch, N. *J. Chem. Phys.* **2002**, *117* (12), 5607−5616.

(104) Lappe, J.; Cave, R. J.; Newton, M. D.; Rostov, I. *J. Phys. Chem. B* **2005**, *109*, 6610−6619.

(105) Stuchebrukhov, A. A. *Chem. Phys. Lett.* **1994**, *225* (1−3), 55−61.